Printed in U.S.A.

78-GT-3

an ASME publication

Performance Investigations of Large Capacity Centrifugal Compressors

H. MISHINA

Senior Researcher,
Mechanical Engineering Research Lab.

I. GYOBU

Senior Engineer

Tsuchiura Works,
Hitachi, Ltd.,
Tsuchiura, Ibaraki, Japan

An experimental investigation concerning the optimum relative velocity distribution within impellers, the optimum diffusion ratio of vaned diffusers and the optimum circumferential area distribution, sectional shape of scrolls was carried out using high specific speed shrouded impellers with backward leaning blades. A performance design procedure based on loss analysis and quasi-three-dimensional flow analysis was also developed and modified by introducing experimental results. The design procedure was applied to a 7900-kw four-stage air compressor to demonstrate the usefulness. Field test results of the complete machine showed that the maximum isothermal efficiency was 75 percent with the pressure ratio of 5.96 and the flow rate of 29.3 m^3/s.

Contributed by the Gas Turbine Division of The American Society of Mechanical Engineers for presentation at the Gas Turbine Conference & Products Show, London, England, April 9-13, 1978. Manuscript received at ASME Headquarters November 7, 1977.

Copies will be available until January 1, 1979.

Performance Investigations of Large Capacity Centrifugal Compressors

H. MISHINA **I. GYOBU**

INTRODUCTION

In recent years the unit capacity of multistage centrifugal compressors with intercoolers for large capacity oxygen plants and working air sources has been increasing steadily. High efficiency as well as high reliability have been demanded, because the power consumption directly affects the power per unit flow rate. Also, compactness and light weight have been demanded in view of resource saving and reduction of space. Therefore, a comprehensive investigation has been carried out from the viewpoint of establishing performance design procedures, production systems. With respect to performance investigation, it was experimentally ascertained that high efficiency and compactness could be accomplished by increasing specific speed and replacing a two-dimensional impeller with a three-dimensional impeller. A series of performance design procedures including optimization of main dimensions, performance prediction and flow analysis of each component such as impeller, diffuser and scroll were developed.

Effects of major factors on the performance were thoroughly examined by using the performance design procedure to grasp problems. A number of the systematic experiments using a model test apparatus of single stage were carried out based on the above examination. Finally, the performance design procedure was modified using these experimental results.

A 7900kW centrifugal compressor was designed and tested as an example to demonstrate the usefulness of this performance design procedure.

This paper describes typical results of the performance investigation of each component to attain high efficiency and compactness of large capacity centrifugal compressors.

APPROACH TO HIGH EFFICIENCY AND COMPACTNESS

The limit to the capacity of centrifugal compressors is determined by many factors such as production engineering, production facilities, transportation, cost, etc. If the compact design is successfully achieved, the range of capacity can be expanded using the existing production facilitities. Therefore, high efficiency should be attained considering compactness. There is no appropriate characteristic value expressing the compactness of a centrifugal compressor. The specific diameter showing the size of the impeller tip diameter can be used as such a value when the ratio of the impeller tip diameter to the outer diameter of the compressor is almost constant.

NOMENCLATURE

A = sectional area
B_f = blockage factor
b = width of flow passage
C = absolute velocity
C_p = pressure recovery coefficient
D = diameter
ℓ = blade camber line distance or meridional distance
N = rotational speed
n_s = specific speed $(=\varphi^{\frac{1}{2}}/\psi^{\frac{3}{4}})$
P = total pressure
p = static pressure
Q = flow rate
u = peripheral velocity
w = relative velocity
z = number of blades
α = flow angle from circumferential direction
β = blade angle from circumferential direction
δ = specific diameter $(=\psi^{\frac{1}{4}}/\varphi^{\frac{1}{2}})$
η_{ad} = adiabatic efficiency
η_i = impeller efficiency
η_{is} = total isothermal efficiency
$\triangle\eta_{ad}$ = adiabatic efficiency rise by vaned diffuser
θ_{sc} = angle from discharge of scroll
μ = slip factor (Cu_2/u_2)
ω = loss coefficient relative to $C4^2/2g$
φ = flow coefficient $(=4Q/\pi D_2^2 u_2)$
φ_1 = flow coefficient $(=c_1/u_2)$
ψ = isentropic head coefficient relative to u_2^2/g

<u>Subscripts</u>
0 = suction
1 = impeller inlet or blade inlet
2 = impeller exit
3 = diffuser inlet
4 = diffuser exit
5 = scroll
d = discharge
des = design point
m = meridional
p = pressure side
s = suction side
t = turning
tot = total
u = circumferential

<u>Superscript</u>
$-$ mean value

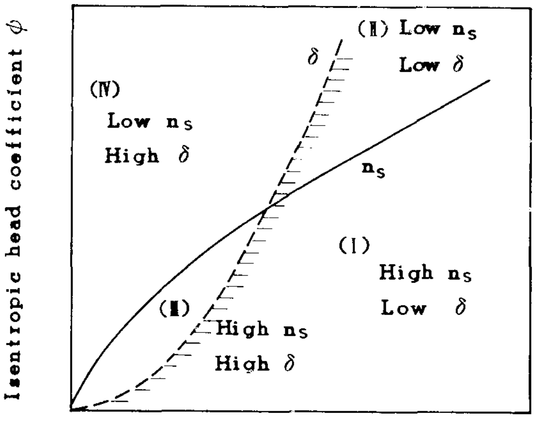

Fig. 1 Relation between specific speed and specific diameter

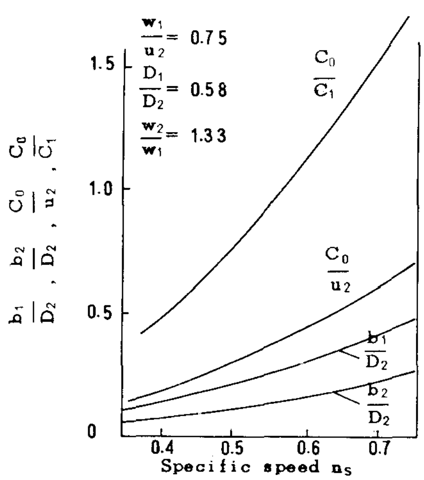

Fig. 2 Meridional velocity and impeller width variation of two-dimensional impeller

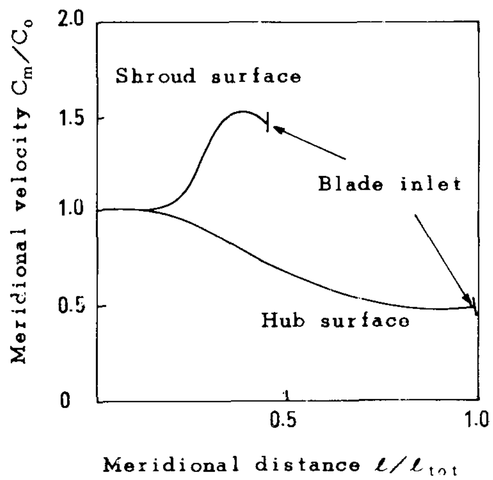

Fig. 3 Meridional velocity distribution at the inlet of two-dimensional impeller

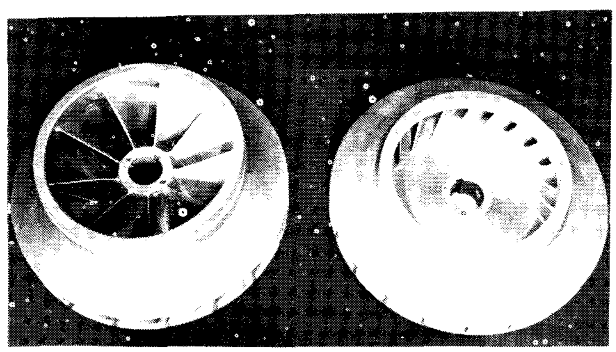

Fig. 4 Two-dimensional (right) and three-dimensional impeller (left)

Fig. 1 shows the relations between isentropic head coefficient and flow coefficient with parameters of specific diameter and specific speed. As can be seen, high efficiency should be attained in the regions (I) and (II). In general, the compact design in case of high specific speed is made by keeping the isentropic head coefficient approximately constant, because the optimum value of isentropic head coefficient for the backward leaning impeller is known.

The points in the compact design of the conventional two-dimensional impeller in case of high specific speed are taken up hereunder. Assuming that the flow downstream of the impeller is constant even though the specific speed varies, the relations between the dimensions and velocities of the impeller are obtained from a one-dimensional analysis.

Fig. 2 shows an example in the case that the diffusion ratio of relative velocity and the inlet diameter ratio are fixed.

As the specific speed increases, the inlet and outlet width ratio of the impeller and the diffusion ratio of the mean meridional velocity of the inlet increase. Moreover, a large difference of velocity occurs on the shroud and hub surface with different curvatures, and flow angles along the both surfaces differ. Accordingly, the flow is separated at the axial symmetric flow passage up to the blade inlet, thus deteriorating the performance. Fig. 3 shows the calculated result of the meridional velocity at the impeller inlet with the specific speed of 0.619. The meridional velocity on the shroud surface is suddenly reduced shortly before the impeller blade inlet after it has been increased once, but the meridional velocity on the hub surface is slowly reduced. Therefore, the flow on the shroud surface differs greatly from that on the hub surface. The incidence angle at the blade inlet is 5 deg. on the shroud surface and 15 deg. on the hub surface. Particularly, the difference between the flow angle and the blade angle is large on the hub surface, and the flow separation occures even though at the design flow rate.

Thus it is clarified that when the compact design using the two-dimensional impeller is made by adopting high specific speed, the blades do not match with the flow and the performance deteriorates. For this reason, it was determined to employ the

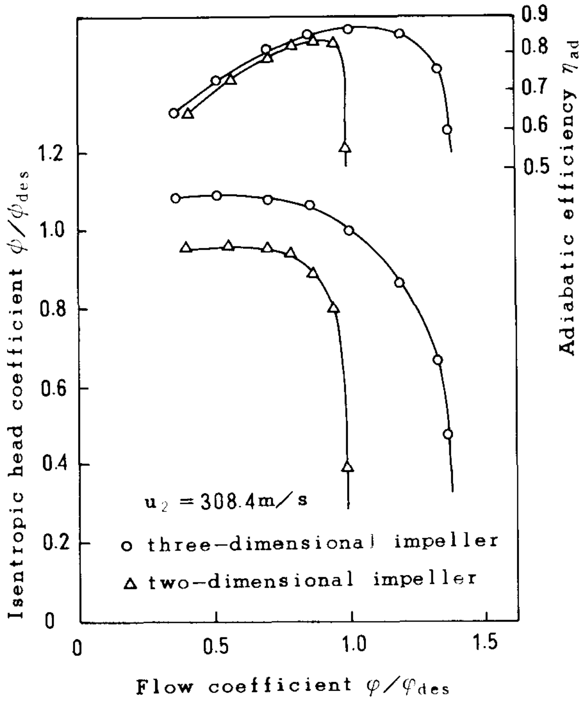

Fig. 5 Performance characteristics of two and three-dimensional impeller

three-dimensional impeller which did not have the axial symmetric flow passage and was provided with the blades twisted three-dimensionally in accordance with the flow.

Fig. 4 shows the photograph of the two-dimensional impeller and the three-dimensional impeller with the same specific speed. Fig. 5 shows the performance characteristics of both impellers combined with the vaneless diffuer and the scroll. The isentropic head coefficient and adiabatic efficiency of the three-dimensional impeller are higher than those of the two-dimensional impeller and the operating range of the former is wide. The three-dimensional impeller is suitable for high efficiency and compact design. Employing the three-dimensional impeller, the adiabatic efficiency is raised by 3 percent and the impeller tip diameter is reduced by 20 percent.

PERFORMANCE DESIGN PROCEDURE

Fig. 6 shows the flow chart of the performance design procedure. A preliminary design is performed by distributing the pressure ratio to each stage for a given specification and optimizing the main dimensions of each component within the required limit e.g., the impeller tip diameter, rotational speed, etc. so that the specification is satisfied and adiabatic efficiency may be maximized. Base on this preliminary design, the performance prediction of each stage is performed and the overall performance is evaluated by accumulating the performance of all stages. If the specification is not satisfied, the limiting conditions are changed and the calculation is repeated until the specification is satisfied. The detailed design of all components is performed by determing the profile of flow passage and obtaining the internal flow. If the flow is not satisfied, the shape of flow passage is corrected.

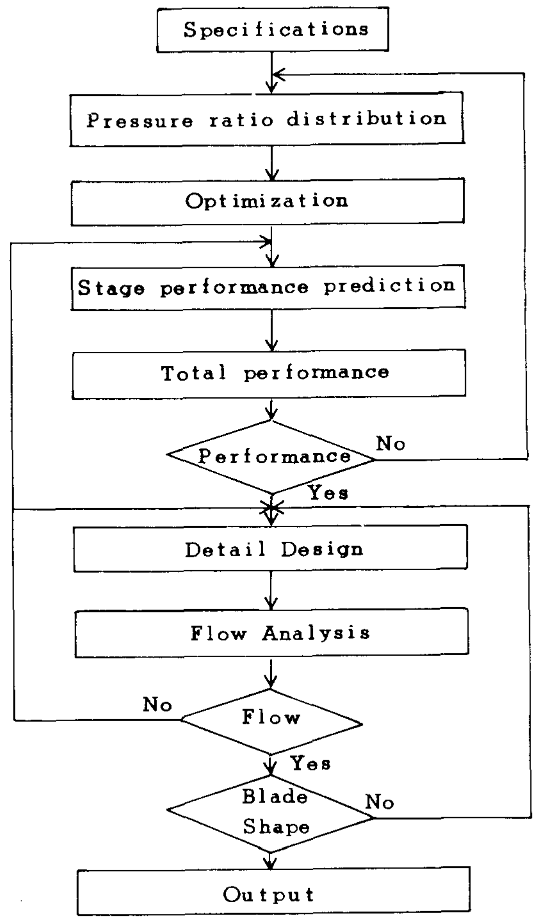

Fig. 6 Flow chart of performance design procedure

If it is necessary to correct the main dimensions which have been optimized, the calculation after performance prediction at each stage is repeated. If the blade shape is not satisfied, the detailed design is repeated. If everything is satisfied, the performance design is finished.

The quality of the design is determined by persons concerned. Therefore, the persons are demanded to have excellent ability of judgement in order to carry out excellent design using this design procedure.

This performance design procedure can be independently used for each calculation block. The loss analysis of each component is required for calculations in optimization of main dimensions and performance prediction. The flow in all components is shown by a simplfied flow model and the loss is formulated in a form containing experimental coefficients. The total loss is obtained by summing up the loss of each component. Losses of each component are presumed as follows (1).

(1) Suction pipe loss
(2) Mixing loss between main flow and leakage flow at the impeller inlet
(3) Impeller internal loss
  Friction loss
  Blade loading loss
  Mixing loss
(4) Impeller external loss
  Disk friction loss

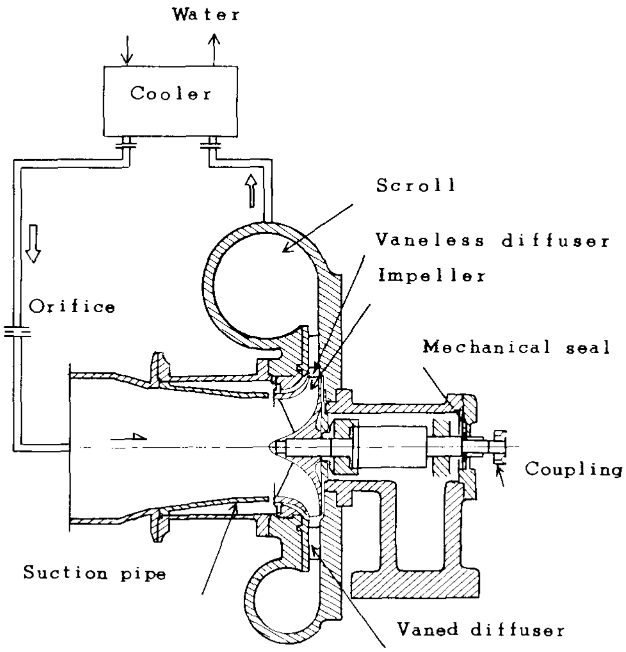

Fig. 7 Model test apparatus

(5) Diffuser loss
Vaneless diffuser loss
Vaned diffuser loss
(6) Scroll loss
(7) Leakage loss

A blockage factor was introduced for the impeller exit and formulated in relation to the impeller internal losses. The Wiesner's (2) formula for the slip factor was used for preliminary calculation and the values obtained from the quasi three-dimensional flow analysis (3) were used in the calculation of performance prediction.

As a result of application of the calculation for performance prediction to the existing centrifugal compressors, it was known that there were several items to clarify the effect on the performance experimentally. The following items are typical ones of each component.

1. The impeller internal loss does not contain a term related to the relative velocity distribution. Therefore, it is necessary to clarify the effect of the relative velocity distribution on impeller efficiency.

2. The vaned diffuser loss contains a term related to the diffusion ratio and the loss coefficient. The loss coefficient employed differs with the shape of the vaned diffuser. Therefore, it is necessary to clarify the effect of the diffusion ratio on the loss coefficient.

3. The scroll loss contains a term related to the circumferential velocity and the loss coefficient. The loss coefficient differs with the scroll shape. Therefore, it is necessary to clarify the effect of the scroll shape on the loss coefficient and the circumferential static pressure distribution.

After the performance design is finished, it can be coupled with the CAD/CAM system which prepares arrangement sheets, machining drawings and program tapes for a numerically-controlled machine tool.

EXPERIMENTAL APPARATUS AND MEASURING METHOD

Experimental apparatus

The experimental apparatus consisted of a test centrifugal compressor, torque meter, DC motor incorporating setup gears, cooler and air piping. A closed circuit of piping was employed to change suction pressure and temperature.

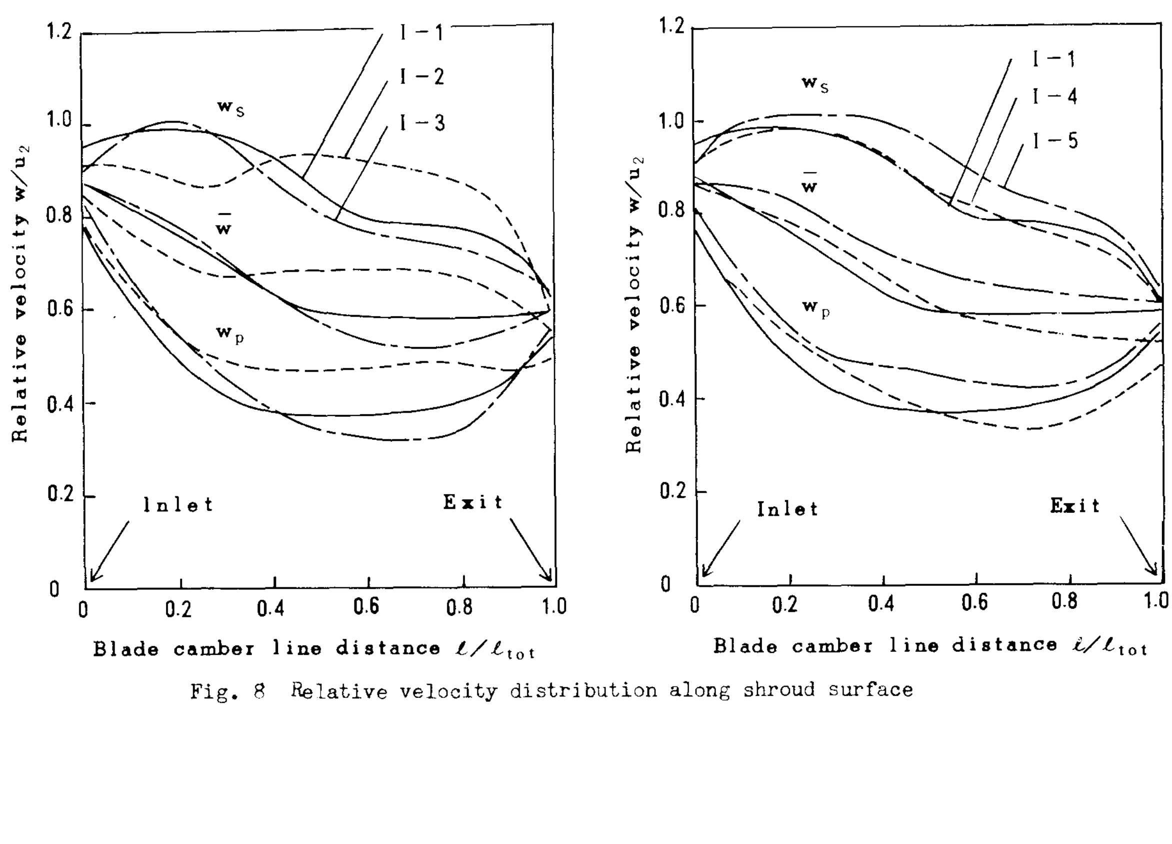

Fig. 8 Relative velocity distribution along shroud surface

Fig. 7 shows the sectional view of the test centrifugal compressor. Various diffusers and scrolls could be attached to the down-stream section of the impeller in accordance with respective purposes. The external surfaces of diffuser and scroll were covered with insulating material to eliminate the heat leakage effect on the total temperature.

Measuring methods

The performance of the centrifugal compressor was obtained by measuring the total pressure, static pressure and total temperature at the suction and discharge measuring sections using Kiel probes, wall pressure taps and copper-constantan thermocouples.

Particularly at the discharge measuring section, the measuring points were increased in view of the flow distortion.

The total pressure, velocity and flow angle were measured at three circumferential positions of the impeller exit, diffuser exit and scroll using cobra type yawmeters to evaluate the performance of each component and know internal flow.

The flow rate was controlled with the valve at the discharge side and measured with an orifice type flow meter in the suction pipe line. Measured data were on-line processed by a data acquisition apparatus using a mini-computer.

Test impellers

Test impellers were shrouded and had eighteen backward leaning blades. The tip diameter was 250 millimeter, the exit blade angle was 75 deg., and the specific speed was 0.587.

EXPERIMENTAL RESULTS AND DISCUSSION

Impeller relative velocity distribution

The effect of relative velocity distribution within the impeller on the performance is a very important problem to design the impeller. This problem was investigated by several researchers (4,5), and the critical diffusion ratio of 1.7 - 2.0 was proposed. However, since the data of the shrouded impeller was less available and the effect in the process of diffusion were not clear, it was decided to carry out a systematic experiment.

The relative velocity distribution on the shroud surface was considered to be most important. Therefore, an experimental investigation using five backward leaning impellers with different relative velocity distributions along the shroud surface was carried out.

Fig. 8 shows the relative velocity distributions along the shroud surface calculated by the quasi three-dimensional flow analysis assuming no internal losses.

The maximum diffusion ratios of the mean relative velocity of the I-1, 2 and 5 impellers are almost equal from 1.47 to 1.54. However, the process of diffusion differs, the diffusion of the I-1 impeller is finished in the first half of the flow passage, the I-2 impeller is diffused near the inlet and exit, and the I-5 impeller is linearly diffused. Though the maximum diffusion ratios of the I-3 and I-4 impellers are almost equal from 1.69 to 1.72, the process of diffusion differs, the diffusion of the I-3 impeller is finished in the first half of the flow passage and accelerated in the second half and the I-4 impeller is linearly

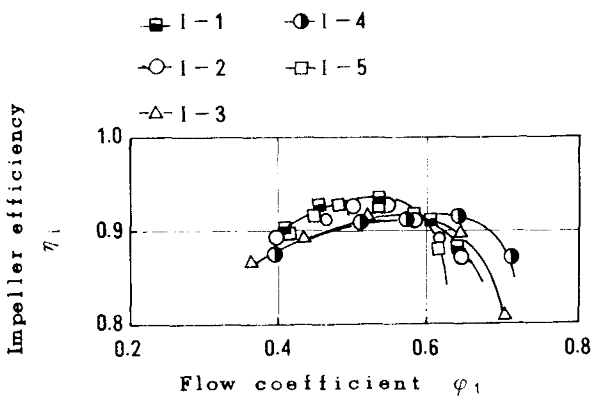

Fig. 9 Impeller efficiency

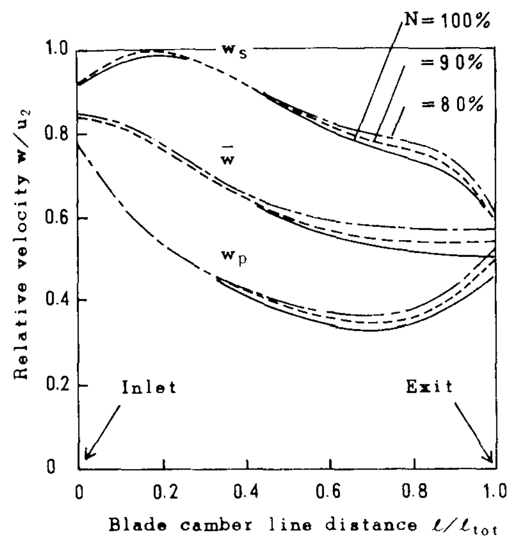

Fig. 10 Relative velocity distribution along shroud surface (I-4 Impeller)

diffused. The diffusion ratios of relative velocity along the suction surface of all impellers are kept almost constant from 1.45 to 1.59.

Fig. 9 shows the impeller efficiency of each impeller combined with the vaneless diffuser of 1.75 radius ratio and the scroll. The impeller efficiency of the I-1, 2 and 5 impellers is generally high, and that of the I-3 and 4 impellers is low. Comparing the efficiency of the I-4 impeller with that of the I-1 impeller, at the design flow rate the efficiency of the former is approximately 3 percent lower than the latter and the maximum efficiency is approximately 2 percent lower than the latter.

When the rotational speed is varied, the specific volume at the impeller exit is varies. Consequently, the diffusion ratio may be varied.

Fig. 10 shows the relative velocity distribution of the I-4 impeller when the rotational speed is varied from 100 percent to 80 percent. When the rotational speed is 80 percent, the maximum diffusion ratio becomes almost equal to that of the I-1 impeller.

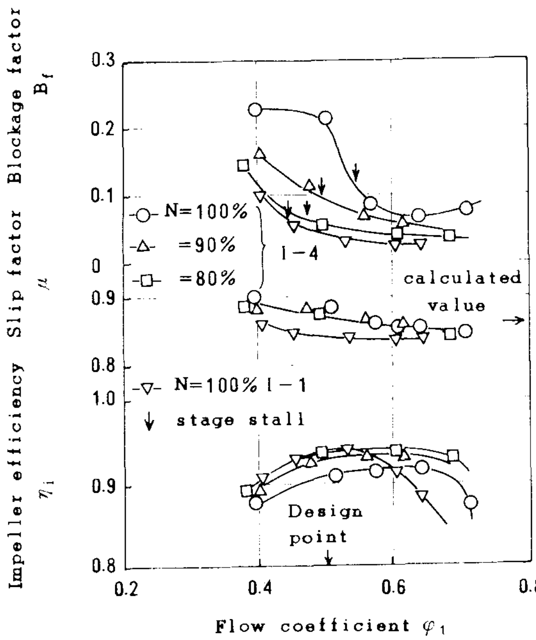

Fig. 11 Impeller performance (I-1, 4 Impeller)

The stage stall is also shown in the figure. Though the blockage factor at the stage stall does not show a constant value, the stage stall is shifted to the lower flow rate as the diffusion ratio decreases. It is clear that the stage stall has a strong relation to the diffusion ratio (6). Fig. 12 shows the flow distribution at the impeller exit of the I-4 impeller at the design flow rate, it indicates that the entire flow deviates to the hub side and there is a large loss at the shroud side. This tendency becomes more remarkable, since the maximum diffusion ratio becomes large and the loss increases when the flow rate decreases.
Also it is indicated that the flow of the shroud side is improved and the loss decreases as the rotational speed decreases and the maximum diffusion ratio decreases.

The flow distribution at the 80 percent rotational speed is considerably similar to that in case of the I-1 impeller shown with a dotted line. The impeller efficiency is roughly determined by the maximum diffusion ratio of the mean relative velocity, and the critical value is from 1.55 to 1.60. The diffusion process of the relative velocity does not greatly affect the impeller efficiency. However, when the impeller is diffused as soon as possible within the critical value and maintained at a low level, the friction loss decreases and the impeller efficiency slightly increases.

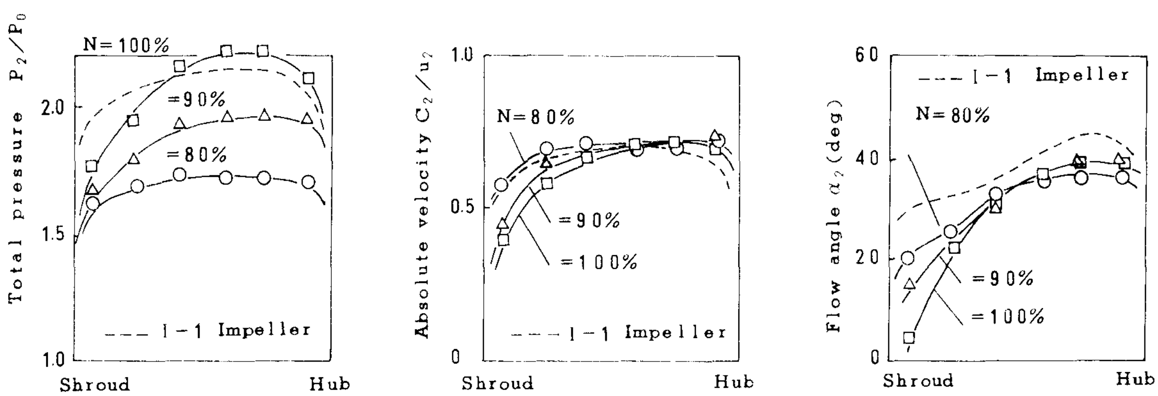

Fig. 12 Flow distribution at impeller exit (1-4 Impeller θ_{sc} = 225 deg.)

Fig. 11 shows the impeller efficiency, slip factor and blockage factor of the I-4 impeller together with those of the I-1 impeller when the rotational speed is varied. When the rotational speed is low and the diffusion ratio of the relative velocity is low, the impeller efficiency increases and is almost equal to that at the 80 percent rotational speed. The slip factor is not affected by the rotational speed. The calculated value by the quasi three-dimensional flow analysis and the experimental value of the slip factor of both impellers are comparatively well coincided.

The blockage factor is strongly related to the impeller efficiency and increases as the impeller efficiency decreases. Since the blockage factor indicates the boundary layer development, flow distortion at the impeller exit, increase of the blockage factor indicates that a large loss occurs due to the boundary layer development and a resulting secondary flow within the impeller and the flow is distorted.

Diffusion ratio of vaned diffuser

With respect to the effect of dimensions on performance of the conventional vaned diffuser, a number of experimental investigations have been carried out, and it was published by Sakurai (7) that there was the optimum relation between the equivalent enlargement angle and length ratio.

The diffusers used in the investigation had circular arc blades with constant thickness, and the experiments were carried out with a low Mach number. The blade thickness distribution and compressibility may affect the optimum value of the vaned diffuser in some cases. Therefore, it was decided to carry out the experiments mainly concerning the diffusion ratio.

Table 1 shows the dimensions of vaned diffusers which were used in the experiments. The blade profile of these vaned diffusers was the NACA65 series.

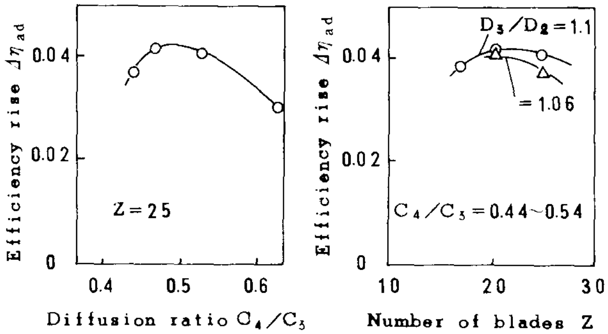

Fig. 13 Adiabatic efficiency rise by diffusion ratio and number of blades of vaned diffusers

The diffusion ratios of the D-1, 2, 3 and 4 diffusers differ. The diffusion ratios of the D-1, 5 and 6 diffusers are almost equal and the number of blades differ. The D-7 and 8 diffusers have small inlet radius ratio of 1.06 and different numbers of blades.

Fig. 13 shows the adiabatic efficiency rise by the vaned diffuser at the design flow rate. In case of the D-2 diffuser, the adiabatic efficiency rise is highest, and in case of the D-4 diffuser it is lowest. The effect of diffusion ratio is remarkable and the effect of the number of blades is relatively small as far as experimented. The optimum value of diffusion ratio is from 0.45 to 0.5 and almost equal to that in case of a low Mach number.

When the number of blades is small, the performance characteristics tended to deteriorate at lower flow rates and become high at higher flow rates.

Fig. 14 shows the static pressure distribution of the D-1 diffuser. The vortex flow from the impeller changes into the two-dimensional channel flow, and the pressure recovery is smoothly carried out in the diffuser channel at the design flow rate. At the lower flow rate, the flow is slightly separated on the suction surface near the inlet, and the pressure recovery along the suction surface is low because of the boundary layer development. However, at the higher flow rate the flow is separated on the pressure surface near the inlet, and the pressure recovery is low through the diffuser.

Circumferential area distribution and cross sectional shape of scroll

The flow in the scroll is very complex and three-dimensional. The approximation of a simple flow model is not sufficient for the loss analysis. Therefore, it was decided to introduce the experimental coefficient and obtain the loss from the systematic experiments. Since the distortion of circumferential static pressure by the scroll affects the upperstream flow i.e., the flow of the diffuser and impeller in case of the vaneless diffuser stage, the circumferential static pressure distribution was also examined.

Fig. 15 shows the circumferential area distribution and cross sectional shape of scrolls used in the experiments.

Table 1 Dimensions of vaned diffusers

	C_4/C_3	Z	D_3/D_2	β_3(deg)	β_4(deg)
D-1	0.44	25	1.1	27.3	47.0
2	0.47	25	1.1	27.3	44.1
3	0.53	25	1.1	27.3	39.4
4	0.63	25	1.1	27.3	31.2
5	0.54	21	1.1	27.3	39.4
6	0.54	17	1.1	27.3	39.4
7	0.45	25	1.06	27.3	41.7
8	0.44	21	1.06	27.3	45.2

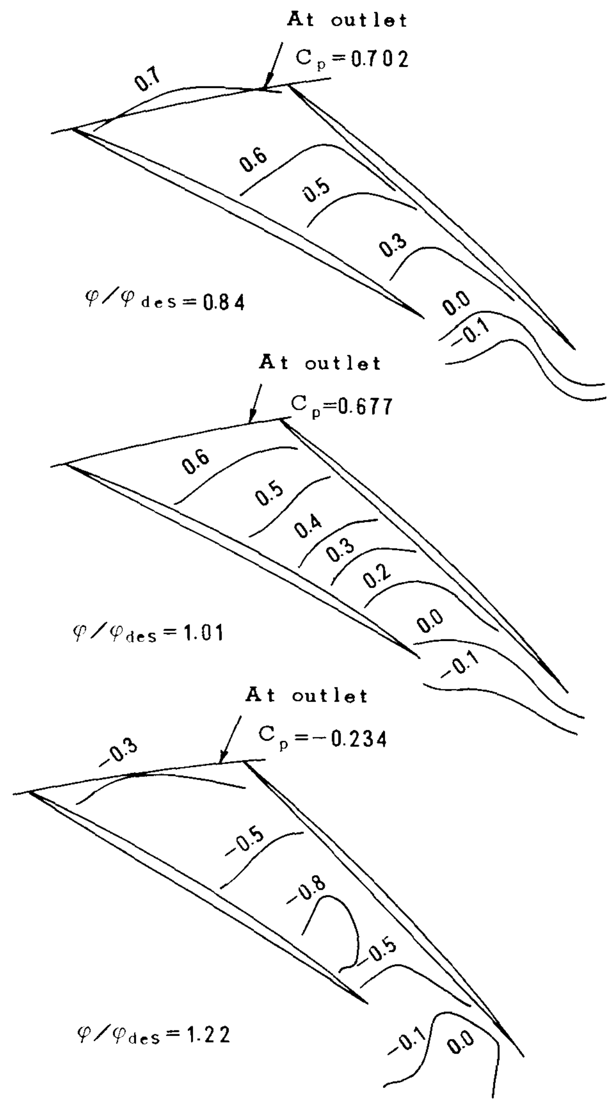

Fig. 14 Pressure distribution of D-2 vaned diffuser

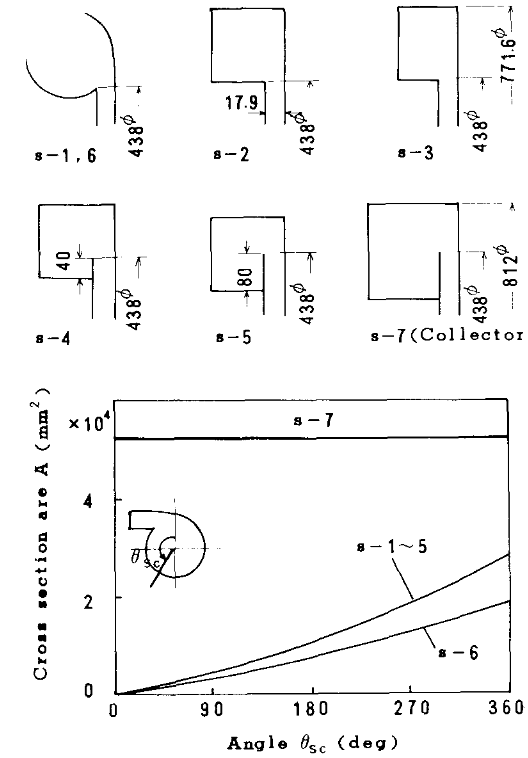

Fig. 15 Circumferential area distribution and cross sectional shape of scrolls

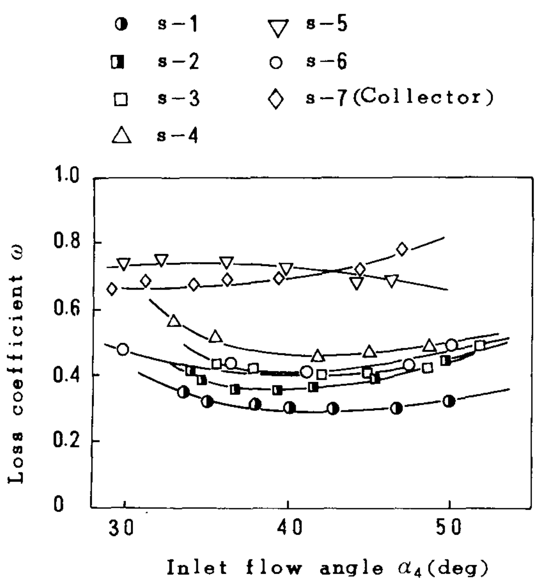

Fig. 16 Loss coefficient of scrolls

The circumferential area distributions of the S-1, 2 and 3 scrolls and determined so that the total pressure loss is minimized, and the S-1 scroll has a circular section, the S-2 scroll has a square section and the S-3 scroll has a rectangular section. The S-4 and 5 scrolls have the same circumferential area distribution, cross sectional shape and different center diameters. The circumferential area distribution of the S-6 scroll is determined assuming that the angular momentum at the diffuser

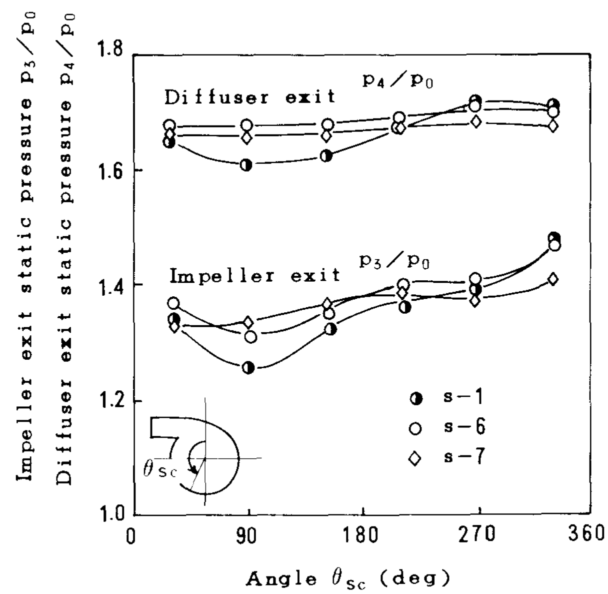

Fig. 17 Circumferential static pressure distribution

outlet is kept in the scroll.

Fig. 16 shows the loss coefficient of scrolls. The loss coefficient of the S-1 scroll is lowest, and that of the collector is highest. Though the effect of the cross sectional shape is relatively small, the circumferential area distribution and the center diameter of the scroll greatly affect the loss coefficient. The value of loss coefficient of the S-5 scroll having a small center diameter is almost equal to the value of the collector.

Fig. 17 shows the circumferential static pressure distribution at the impeller and diffuser exit at the design flow rate of the S-1, 7 scrolls and the collector. The circumferential static pressure distribution of the S-1 scroll is not uniform as compared with the S-7 scroll and the collector, and increases in the flow direction along the scroll. This tendency appears remarkably at the impeller exit. However, such a circumferential static pressure distribution had no effects on the stage stall as far as experimented.

Fig. 18 shows the velocity distribution in the S-1 and 6 scrolls at the design flow rate. The circumferential velocity is almost uniform in the axial direction except at the angle of 90 deg., and decreases as the radius increases in the radial direction. Though the general tendencies of flows in both scrolls are similar, the velocity level is low in case of the S-1 scroll with a large sectional area near the discharge side. The flow in the cross section of the scroll rotates around the center of the section and is diffused in the rotational direction. Particularly, at the section of the angle of 360 deg., the diffusion in the rotational direction is remarkable.

A strong vortex flow from the diffuser exit is gradually diffused as it rotates around the center, and goes in the circumferential direction up to the discharge as it is diffused.

The loss of the scroll becomes low when the flow is diffused so that the total of wall friction and mixing loss is minimized.

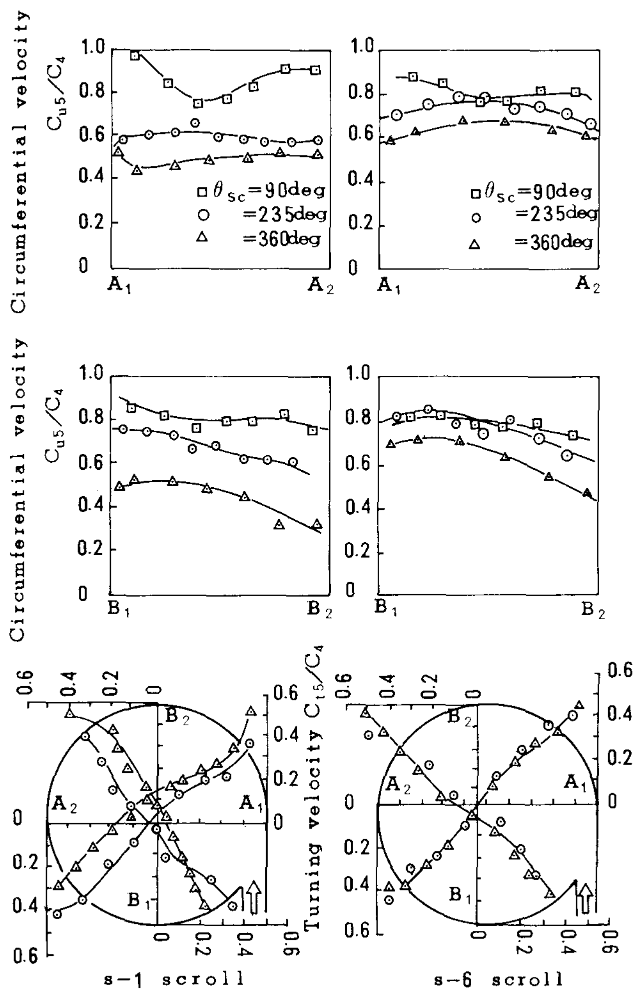

Fig. 18 Velocity distribution in scrolls at the design flow rate

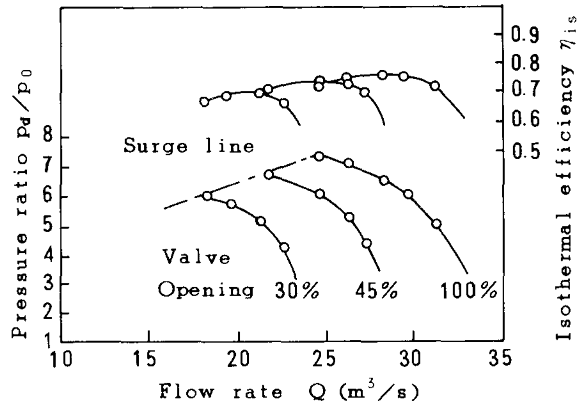

Fig. 19 Over-all performance characteristics

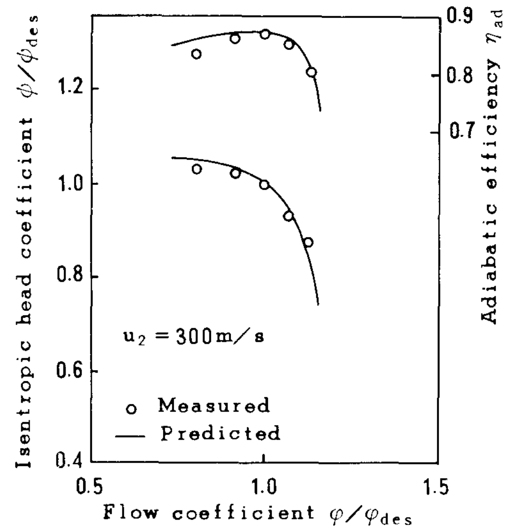

Fig. 20 Comparison of measured and predicted performance characteristics of first stage

Table 2 Specifications of 7900kW Air Compressor

Items	Specifications
Type	2 Shafts 4 Stages
Flow rate	28.01 m^3/s
Suction pressure	1.013 kg/cm^2 abs
Discharge pressure	5.883 kg/cm^2 abs
Suction temperature	30℃
Gas handled	Air
Motor power	7900kW 6p 60HZ

APPLICATION TO A 7900 kW CENTRIFUGAL COMPRESSOR

The performance design procedure was applied to a 7900 kW two-shaft, four-stage centrifugal compressor to demonstrate the usefulness.

Table 2 shows the design specifications of this centrifugal compressor.

Fig. 19 shows the performance characteristics obtained from field tests with a parameter of suction valve opening. As can be seen, a very flat efficiency characteristic having a wide operating range was obtained. A high isothermal efficiency of 75 percent was obtained at the design flow rate. This efficiency is of the world's highest level for same capacity centrifugal compressors. The mechanical tests were fully satisfactory. The machine had a vibration level of the shaft of from 10 to 15 μm double amplitude. The noise level was from 80 to 85 dB (A) with an insulating hood.

Fig. 20 shows the comparison between the predicted and measured values of the first-stage performance characteristics. Both values comparatively well coincide, and the usefulness of the performance design procedure at the complete machine was ascertained.

Based on these test results, the two-shaft, four-stage centrifugal compressors covered by the thirteen sizes were put on the market.

The capacity range could be expanded up to 107.4 m^3/s with the pressure ratio from 5 to 7.

CONCLUSIONS

For the purpose of high efficiency and compactness of large capacity centrifugal compressors, an experimental investigation of each component was carried out. The following conclusions were obtained.

1. Impeller efficiency was roughly determined by the maximum diffusion ratio of the mean relative velocity, and the critical value was from 1.55 to 1.6. The optimum relative velocity distribution was a combination with the rapid diffusion within the critical value and gradual acceleration.
2. Vaned diffuser efficiency was mainly determined by the diffusion ratio. The optimum value was from 0.45 to 0.5, and almost equal to that in case of a low Mach number.
3. Scroll loss was mainly determined by the circumferential area distribution and the center diameter. The optimum circumferential area distribution was determined so that the total of wall friction and mixing loss was minimized.
4. These experimental results were introduced in the newly developed performance design procedure including optimization, performance prediction and flow analysis of each component.
5. Field test results of a 7900 kW four-stage air compressor showed that the maximum isothermal efficiency was 75 percent with the pressure ratio of 5.96 and the flow rate of 29.3 m^3/s.

ACKNOWLEDGMENTS

The authors wish to express their appreciation to Mechanical Engineering Research Laboratory and Tsuchiura Works for permission to publish this paper.

They also thank Mr. H. Nishida, Mr. K. Naya and Mr. F. Koseki for their technical assistance and experimental work during carrying out this investigation.

REFERENCES

1. Jansen, W., "A method for Calculating the Flow in a Centrifugal Impeller when Entropy Gradients are Present," Internal Aerodynamics, IME, Paper 12, 1970, pp. 133 - 146.
2. Wiesner, F.J., "A Review of Slip Factors for Centrifugal Impellers, "Journal of Engineering Power, Trans, ASME, Series A, Vol. 89, No. 4 Oct. 1967, pp. 558 - 572.
3. Senoo, Y., and Nakase, Y., "An Analysis of Flow Through a Mixed Flow Impeller," Journal of Engineering for Power, Trans. ASME, Series A, Vol. 94, 1972, pp. 43 - 50.
4. Dallenbach, F., "The Aerodynamic Design and Performance of Centrifugal and Mixed-Flow Compressors," SAE Technical Progress Series, Vol. 3, 1961, pp. 2 - 30.
5. Dean, R.C. Jr., "The Fluid Dynamic Design of Advanced Centrifugal Compressors," Creare TN - 185, Jul. 1974.
6. Rodgers, C., "Impeller Stalling as Influenced by Diffusion Limitations," Centrifugal Compressor and Pump Stability, Stall and Surge, ASME, New York, 1976, pp. 37 - 67.
7. Sakurai, T., "Flow Separation and Performance of Decelerating Channels for Centrifugal Turbomachines," Journal of Engineering for Power, Trans. ASME, Series A, Vol. 97, No. 3, Jul. 1975, pp. 388 - 394.